NASA Technical Memorandum 81285

Full-Scale Aerodynamic Characteristics of a Propeller Installed on a Small Twin-Engine Aircraft Wing Panel

Philip R. Barlow, Victor R. Corsiglia, and Joseph Katz

May 1981

National Aeronautics and Space Administration

NASA Technical Memorandum 81285

Full-Scale Aerodynamic Characteristics of a Propeller Installed on a Small Twin-Engine Aircraft Wing Panel

Philip R. Barlow
Victor R. Corsiglia
Joseph Katz, Ames Research Center, Moffett Field, California

National Aeronautics and
Space Administration

Ames Research Center
Moffett Field, California 94035

NOMENCLATURE

c	blade chord
C_D	drag coefficient
C_ℓ	sectional lift coefficient of propeller blade
C_P	power coefficient, $\frac{\text{power}}{\rho n^3 D^5}$
C_{P_U}	upper-plenum pressure coefficient
C_T	thrust coefficient, $\frac{T_h}{\rho n^2 D^4}$
D	propeller diameter, 1.93 m (6.3 ft)
D_s	spinner diameter, 0.37 m (1.2 ft)
J	advance ratio, $\frac{V_\infty}{nD}$
L/D	lift/drag ratio
M_T	blade-tip Mach number
n	propeller revolutions/sec
p	total pressure
q	free-stream dynamic pressure, $\frac{\rho V_\infty^2}{2}$
r	propeller radius
Re	Reynolds number
S	reference area
t	blade thickness
T_h	propeller thrust
T_o	propeller shaft torque
V_∞	free-stream tunnel speed, m/s
α	angle of attack, deg
β	blade incidence angle at 3/4-blade radius, deg

η propeller efficient, $\frac{C_T J}{C_p}$

ρ air density

FULL-SCALE AERODYNAMIC CHARACTERISTICS OF A PROPELLER INSTALLED ON A SMALL TWIN-ENGINE AIRCRAFT WING PANEL

Philip R. Barlow, Victor R. Corsiglia, and Joseph Katz*

Ames Research Center

SUMMARY

Full-scale measurements of shaft thrust and torque were made in a wind tunnel on a typical small twin-engine aircraft propeller mounted on a wing. Wind-tunnel speeds and blade angles were set for full-scale flight conditions. Excellent quality measurements were obtained of the thrust coefficient, the power coefficient, and the propeller efficiency for various values of the advance ratio and the blade incidence angle at 3/4-blade radius. A conventional propeller theory found in the literature was applied to the present results. Although thrust, power, and efficiency were somewhat overpredicted, the advance ratio for maximum efficiency was predicted quite accurately. It was found that, for some conditions, spinner drag could be significant. A simple correction that was based on the spinner base pressure substantially accounted for the changes in efficiency that resulted from this cause.

INTRODUCTION

During recent cooling drag investigations conducted in the NASA-Ames 40- by 80-Foot Wind Tunnel, propeller thrust and torque measurements were made on a typical two-bladed propeller at full-scale flight conditions. The primary objective of these measurements was to define realistic cruise and climb conditions to be used in a study of cooling drag (see refs. 1-3). These same propeller measurements are, however, of considerable interest because of the scarcity of measurements on the performance of installed propellers. In addition to a presentation of these measurements in this paper, a spinner-drag correction is described and comparisons are made with a conventional propeller theory.

EXPERIMENTAL APPARATUS

Figure 1 shows the semispan wing mounted vertically on an end plane in the NASA-Ames 40- by 80-Foot Wind Tunnel. The wing, which was from the left side of a Piper Seneca II airplane, was kept at 0° angle of attack throughout the propeller portion of the study. Additional details of the experimental

---

*National Research Council Fellow, Moffett Field, Calif. 94035. Now Professor, Mechanical Engineering Dept., Technion, Haifa, Israel.

setup are described in references 1-3. Figure 2 is a sketch of the nacelle internal arrangement. The propeller is driven by an electric motor through a torque-thrust meter. Propeller blade pitch was held fixed by an adjustable mechanical device that replaced the production constant-speed mechanism that is normally mounted on the propeller. Blade pitch angle was measured at the 3/4-blade radius with a bubble protractor on the lower surface of the blade section. Angles were set to within ±1/4°. The rpm (revolutions per minute) was measured with the aid of a magnetic pickup on the drive shaft.

The cooling airflow that was being studied in the cooling drag portion of the study was ducted from the inlets, as shown in figure 1, to the upper plenum, as shown in figure 2. Air passed through the adjustable orifice plate, which simulated the resistance of the cooling fins of a gasoline engine to the lower plenum. The air then exited via a cowl flap. The orifice opening and the cowl-flap setting were held fixed during the propeller portion of the study so that a flow rate representative of a cruise condition was simulated. Total pressure as recorded in the upper plenum was used in the present study as a measure of the back pressure on the propeller spinner.

The propeller [Hartzell 8459-8R (D = 1.93 m (6.3 ft))] is the one that is normally installed on this wing. The blade section was a Clark-Y inboard and an RAF 6 from about 63% blade radius to the tip. Figure 3 shows the twist, maximum thickness, and chord variation as functions of blade radius. The continuous curve was supplied by the manufacturer and the data points were obtained from a survey of the blade geometry by using a machinist's flat table, distance gages, and calipers. The activity factor was calculated by using the following expression:

$$AF = \frac{100,000}{16} \int_{0.15}^{1} \frac{c}{D} x^3 \, dx$$

which yields AF = 111.

The torque-thrust meter was identical to the one used by NASA-Langley Research Center in their Advanced Technology Light Twin Program (see ref. 4). The meter consisted of four uniformly spaced radial flexures with strain gages attached to measure the torque and thrust simultaneously. The meter was attached between the motor shaft and the propeller. Slip rings that conducted the measured signals to the data-acquisition system were air cooled.

Calibration and Equations for the Torque-Thrust Meter

A calibration of the torque-thrust meter was performed in a balance calibration lab prior to installation in the wing. A special machine was used to load the meter separately in thrust and torque (without rotation). Figure 4 shows the voltage signals from each channel with both thrust only and torque only applied. As can be seen, there is excellent linearity and no hysteresis on the thrust and torque output when loaded in thrust and torque, respectively.

The interaction between gages is 6% and 2% for thrust and torque, respectively. Some hysteresis can be seen in the interactions.

The interactions were accounted for in the data reduction by using the following data-reduction equations:

$$\text{Thrust (lb)} = K_1 Th(mV) - K_2 T_Q(mV)$$

$$\text{Torque (in.-lb)} = K_3 Th(mV) - K_4 T_Q(mV)$$

where $K_1 - K_4$ were obtained from the four measured slopes shown in figure 4 according to the equations

$$K_1 = \frac{a_{22}}{DET} \qquad K_2 = \frac{a_{12}}{DET} \qquad K_3 = \frac{a_{11}}{DET} \qquad K_4 = \frac{a_{21}}{DET}$$

where

$$DET = a_{11}, a_{22} - a_{12}\, a_{21}$$

Propeller Calibration Procedure

The values of blade pitch angle and advance ratio to be used later in the cooling drag study were selected to be in the vicinity of the two operating points of interest. Values of these points, which are cruise and climb, are given in Table 1. The angle of attack of the wing was held fixed at 0°; thus four blade-angle settings were used. Values of the propeller parameters for each of the four blade-angle settings are given in Table 2. The test procedure was to set blade pitch angle and tunnel speed and then vary the rotational speed to obtain the desired values of advance ratio.

RESULTS

Thrust, Power, and Efficiency

The measured power coefficient and efficiency as functions of advance ratio (J) and blade pitch angle (β) are shown in figure 5. These curves were obtained by interpolating and extrapolating the measured data by using the propeller theory described in the following section as a guide. Also shown are the cruise and climb points. As can be seen, an efficiency of about 79% was obtained near the cruise condition. For climb, the efficiency was $\eta = 73\%$. As can be seen in figure 6, efficiency declines gradually to $\eta = 70\%$ as J is varied for constant β and declines rapidly beyond $\eta = 70\%$.

The thrust measurements obtained on the shaft balance were compared with those obtained from the wind-tunnel scales by subtracting the propeller-off

drag values as measured on the wind-tunnel scale from the corresponding values when the propeller was operating. This scale-measured thrust includes the interference between the propeller slipstream and the nacelle, whereas the shaft balance measurement does not. As can be seen in figure 7, the wind-tunnel scale-measured thrust is slightly higher; thus a favorable slipstream flow interference on the nacelle is indicated.

Comparison with Theory

Calculations were performed by using a classical vortex theory[1] and comparisons were then made with the present measurements. The method is based on Goldstein's Vortex Theory as discussed in references 5 and 6.

Goldstein replaces each blade with a single radial bound-line vortex. The vorticity gradient along each bound-line vortex forms a vortex sheet that trails behind the propeller in a helix. The vortex sheet induces a velocity in the propeller plane that is normal to the resultant velocity. Studies have indicated that good agreement between experiment and theory is obtained when a normality condition of the induced velocity and resultant velocity at the propeller plane is specified (see ref. 5). This condition was specified for the present treatment. The induced angle of attack can then be computed and a resultant sectional angle of attack calculated. A two-dimensional look-up table for the lift and drag coefficients is referenced and the values are used in a numerical integration for the nondimensional thrust (C_T) and power (C_P) coefficients.

The airfoil sectional lift and drag coefficients used in the code were for a Clark-Y with the effects of Mach number and thickness included. The propeller being studied herein was, however, designed with a Clark-Y section to only 63% blade radius and the outboard sections were approximately RAF-6. Figures 8 show a comparison between the values of C_ℓ found in the literature (refs. 7 and 8) with the values used in the code. The Reynolds number (Re) at the propeller midradius is approximately 1.4 million. Clark-Y sectional data were found for $Re = 0.5$ million and $Re = 3$ million. RAF-6 data were found only for $Re = 0.5$ million. Good agreement can be seen between the values in the code and those found in the literature. Variations of the drag coefficient were found to exist between the values found in the literature and those used by the code, but these variations were found to have only a minor effect upon the resultant values of power coefficient. Also, in the code no provision was made to model the effects of the nacelle or the wing. The spinner drag was computed by using the method described in the following section.

The computed values of thrust and power coefficient are shown in figures 9. As can be seen, the thrust and power coefficients are predicted well at the value of β for maximum efficiency ($\beta = 25°$, fig. 5) and $J \geq 1$. These quantities are generally overpredicted for other values of J and β. The peak efficiency values (fig. 9(c)) are overpredicted by 4 to 8%. However,

---

[1]The assistance of Prof. S. J. Miley, Texas A & M University, in the acquisition of this code and performance of some of the calculations is gratefully acknowledged.

the value of J for maximum efficiency is predicted well. At the condition of maximum efficiency for the 25° blade-angle case, it was noted that the sectional angles of attack along the blade were, for the most part, in a small range about the values of angle of attack that correspond to maximum L/D of the blade section.

Spinner Drag Correction

One interesting trend noted during analysis of the cooling drag results is shown in figure 10 (uncorrected data). At the cruise flight condition (q = 80 psf), propeller efficiency appeared to vary with the upper plenum pressure. It can be seen in figure 2 that the base of the spinner is exposed to the upper plenum pressure. For these data the upper plenum pressure varied because of changes in the flow rate of air through the nacelle caused by changes in the orifice-plate opening and cowl-flap setting (see fig. 2). These changes are, however, unrelated to the propeller performance characteristics. This changing base pressure introduces an extraneous spinner drag, which obscures the propeller characteristics. A correction was therefore derived to account for this changing spinner base pressure. The spinner base pressure is taken to be uniform and equal to the upper plenum pressure, and the frontal pressure is assumed to vary quadratically from stagnation at the nose of the spinner to the base pressure at the aft edge. The resulting spinner drag was, accordingly,

$$\text{Drag}_{\text{spinner}} = \int_0^{D_s/2} \Delta p 2\pi r \, dr$$

where

$$\Delta p = q\left(1 - C_{P_U}\right)\left[1 - \left(\frac{2r}{D_s}\right)^2\right]$$

and D_s (diameter of the spinner) is 0.37 m (1.2 ft). The resulting correction to the thrust coefficient and efficiency is

$$\Delta C_T = \frac{\pi}{16}\left(\frac{D_s}{D}\right)^2 J^2\left(1 - C_{P_U}\right)$$

$$\Delta \eta = \frac{\pi}{16}\left(\frac{D_s}{D}\right)^2 \frac{J^3}{C_P}\left(1 - C_{P_U}\right)$$

It can be seen in figure 10 that the variation in the propeller efficiency with C_{P_U} in cruise is substantially reduced when this correction is applied. For the climb condition, the value of J is such that the resulting correction ($\Delta\eta$) is small.

It should be noted that, during the propeller portion of the study, the upper-plenum pressure varies over a limited range ($0.6 < C_{P_U} < 0.7$, cruise) since the orifice-plate opening and the cowl flap were held fixed. Therefore, the correction had a small effect on these data. The corrected values of C_T are shown in figure 11. It can be seen that the effect of the correction is small.

CONCLUDING REMARKS

Full-scale measurements of shaft thrust and torque were made in a wind tunnel on a typical general-aviation propeller mounted on a semispan wing. Wind-tunnel speeds and blade angles were set for full-scale flight conditions. Excellent quality measurements of C_T, C_P, and η for various values of J and β were obtained. It was found that a maximum efficiency of 79% occurred at the operating point corresponding to cruise. The climb efficiency was 73%. A conventional propeller theory found in the literature and based on the method of Goldstein was applied to the present results. Small overpredictions of thrust and power were obtained that corresponded to about 1.3° of blade pitch angle. Excellent agreement was found, however, for the values of the advance ratio for maximum efficiency for each blade pitch angle. The maximum efficiency values were, however, about 5 to 10% higher than predictions.

It was also found that the spinner drag could be significant for some conditions. Varying the upper-plenum pressure by changing the flow rate of cooling air through the nacelle changed the propeller efficiency. A simple correction was derived that accounted for the varying pressure on the aft surface of the spinner. It was then found that the correction substantially accounted for the variation of propeller efficiency with upper-plenum pressure.

REFERENCES

1. Katz, J.; Corsiglia, V. R.; and Barlow, P. R.: Effect of Propeller Slipstream on the Drag and Performance of the Engine Cooling System for a General Aviation Twin-Engine Aircraft. AIAA Paper 80-1872, Aug. 1980.

2. Katz, J.; Corsiglia, V. R.; and Barlow, P. R.: Study of Cooling Air Inlet and Exit Geometries of Horizontally Opposed Piston Aircraft Engines. AIAA Paper 80-1242, July 1980.

3. Corsiglia, V. R.; Katz, J.; and Kroeger, R. A.: Full Scale Wind Tunnel Study of Nacelle Shape on Cooling Drag. Journal of Aircraft, vol. 18, no. 2, Feb. 1981, pp. 82-88.

4. Fink, M. P.; and Freeman, D. C., Jr.: Full-Scale Wind-Tunnel Investigation of a Static Longitudinal and Lateral Characteristics of a Light Twin-Engine Airplane. NASA TN D-4983, 1968.

5. McCormick, B. W., Jr.: Aerodynamics of V/STOL Flight. Academic Press, 1967.

6. Pauling, David V.: The Effect of Uncertainties on Predicting Rotor and Propeller Performance. AD-A008 419, Pennsylvania State Univ., May 1975.

7. Stack, J.: The N.A.C.A. High-Speed Wind Tunnel and Tests of Six Propeller Sections. NACA TN 463, 1933.

8. Pinkerton, R. M.; and Greenburg, H.: Aerodynamic Characteristics of a Large Number of Airfoils Tested in the Variable-Density Wind-Tunnel. NACA TN 628, 1937.

TABLE 1.- TEST OPERATING CONDITIONS

Parameter	Climb	Cruise
q, cm H_2O (psf)	13.1 (26)	40.3 (80)
V_∞, m/s (knots)	50 (92)	84 (161)
β, deg	18.7	25
η, %	73	79
J	.58	1.06
C_T	.063	.036
C_P	.050	.048

TABLE 2.- PROPELLER DATA

β, deg	V_∞, knots	rpm	J	M_T	C_P	C_T	η,%
15	83.8	2455	0.546	0.728	0.0287	0.0403	76.5
	83.7	2110	.635	.626	.0206	.0241	74.4
	83.5	1763	.758	.524	.0080	.0025	23.8
	83.3	1591	.838	.472	-.0005	-.0109	1804.4
	82.6	1365	.968	.406	-.0206	-.0399	187.3
20	84.5	2463	.549	.732	.0595	.0755	69.7
	83.2	1758	.757	.522	.0392	.0394	76.1
	82.7	1654	.800	.492	.0341	.0318	74.6
	82.9	1541	.860	.438	.0280	.0233	71.7
	81.7	1370	.954	.406	.0144	.0071	47.1
25	81.0	1762	.735	.526	.0863	.0838	71.4
	116.1	2001	.928	.596	.0693	.0576	77.2
	80.9	1365	.948	.406	.0633	.0533	79.8
	115.6	1742	1.061	.518	.0475	.0359	80.3
	115.3	1384	1.333	.400	-.0042	-.0098	309.2
31	100.3	1366	1.174	.406	.0895	.0588	77.2
	100.4	1202	1.336	.356	.0622	.0338	72.6
	100.8	1075	1.500	.320	.0277	.0063	33.9

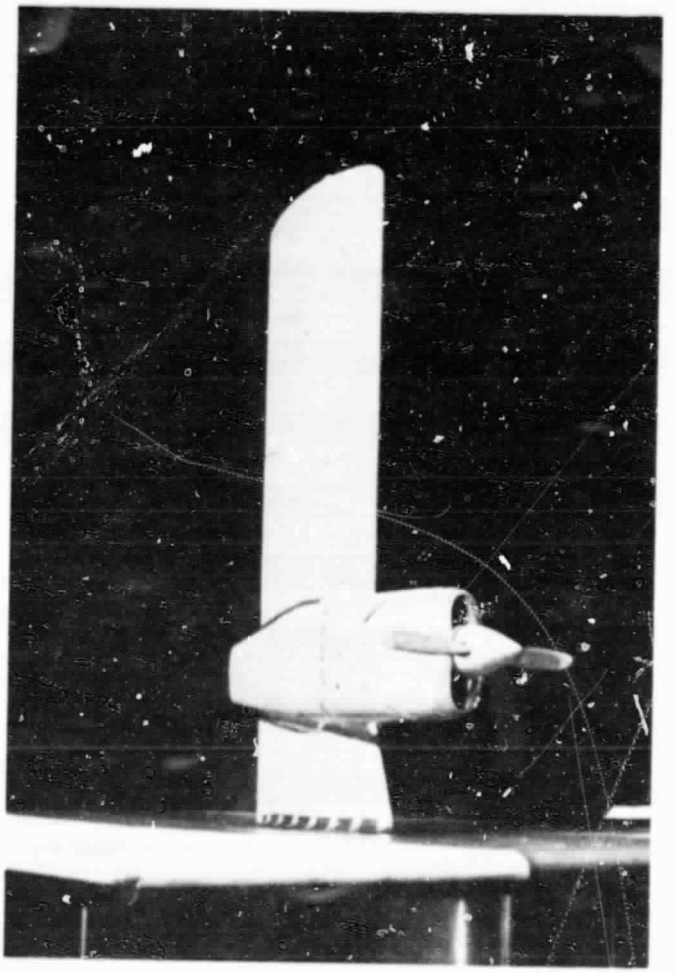

Figure 1.- Propeller and wing installed in the NASA-Ames 40- by 80-Foot Wind Tunnel.

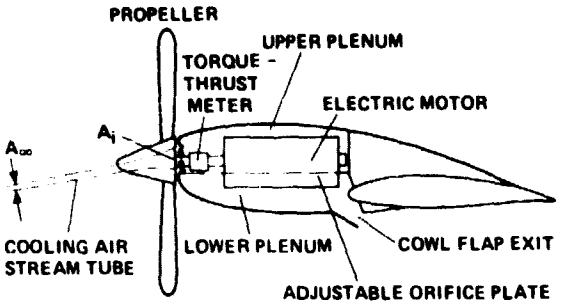

Figure 2.- Schematic drawing of nacelle internal arrangement.

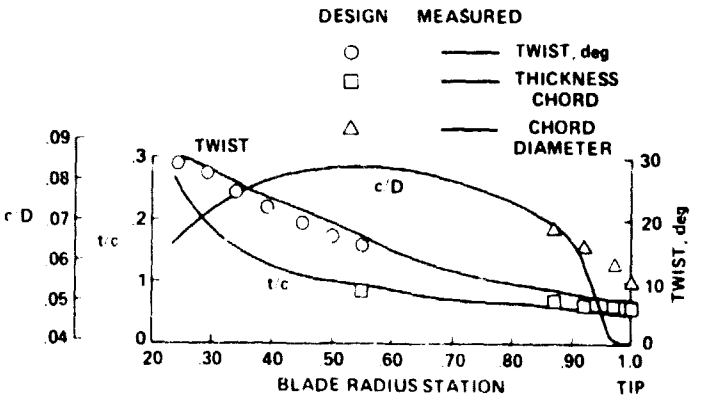

Figure 3.- Geometric characteristics of the propeller obtained from manufacturer and from a bench survey.

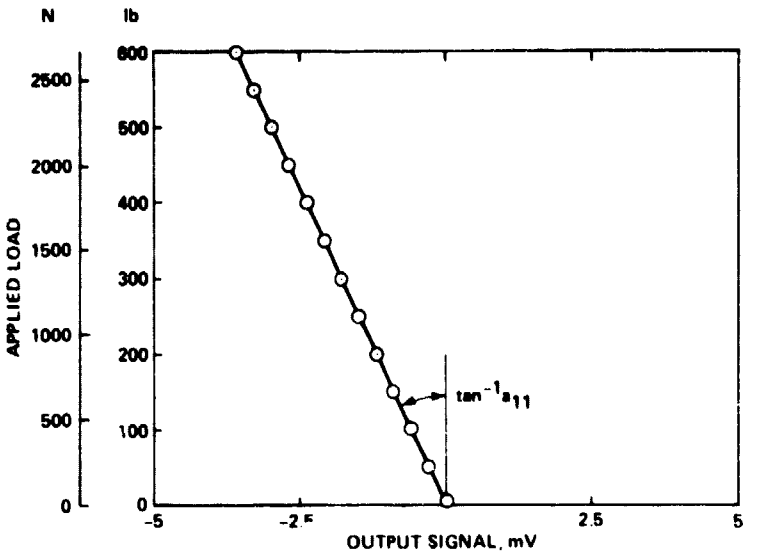

(a) Thrust output, thrust load.

Figure 4.- Torque-thrust meter calibration.

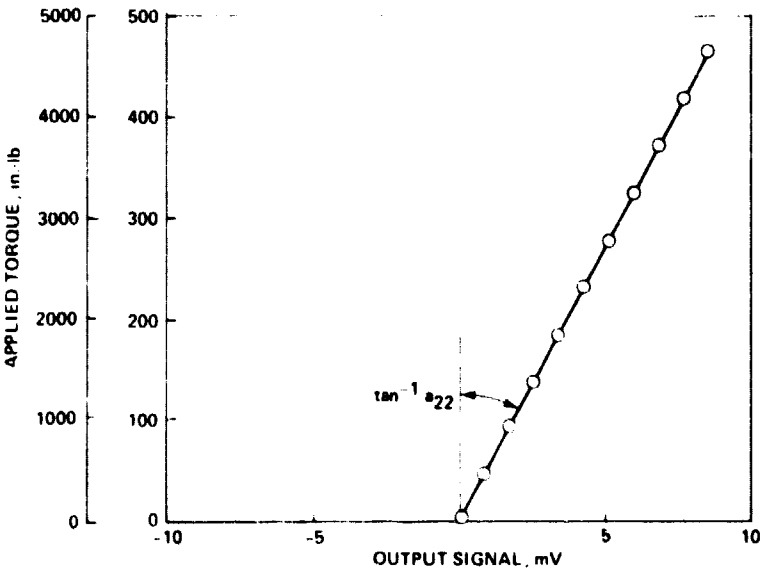

(b) Torque output, torque load.

Figure 4.- Continued.

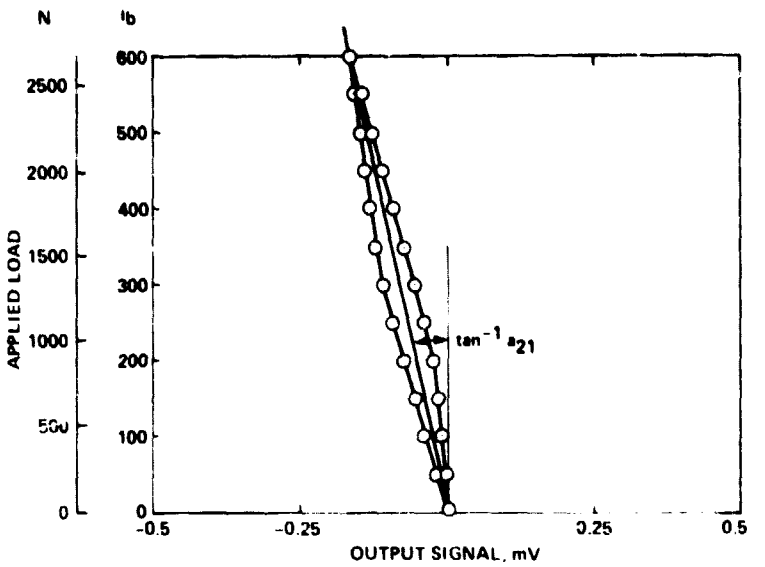

(c) Torque output, thrust load.

Figure 4.- Continued.

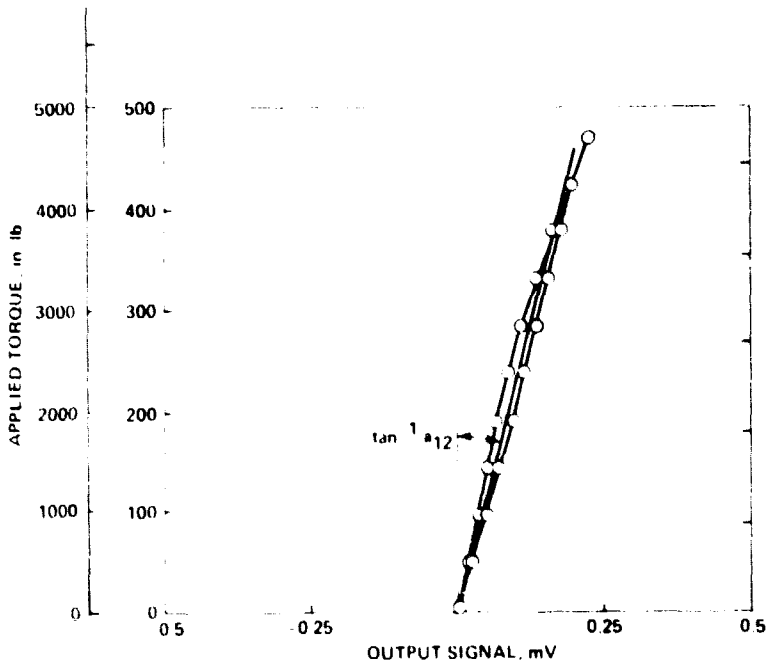

(d) Thrust output, torque load.

Figure 4.- Concluded.

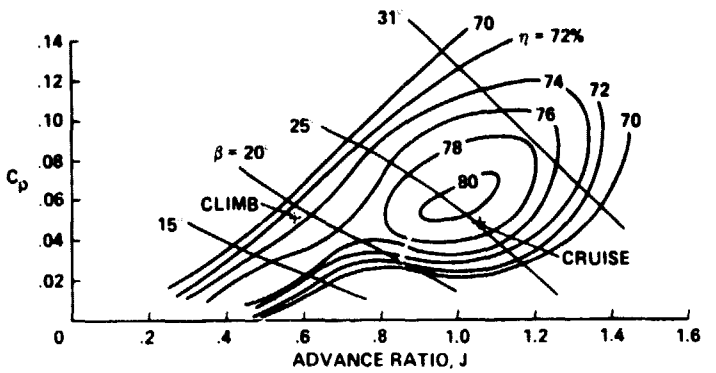

Figure 5.- Measured effect of advance ratio and blade pitch angle on power and efficiency. Note cruise and climb conditions.

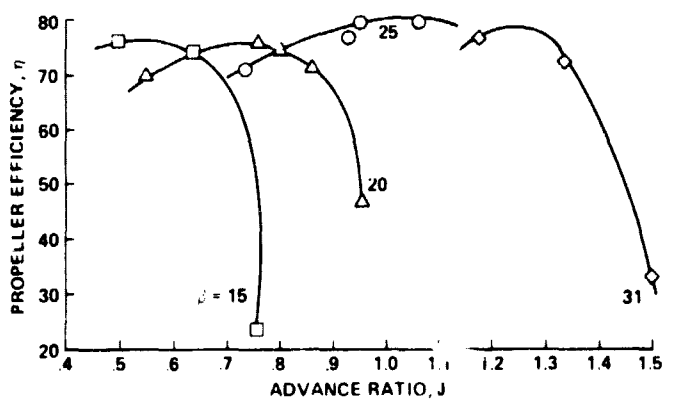

Figure 6.- Measured effect of advance ratio and blade pitch angle on efficiency.

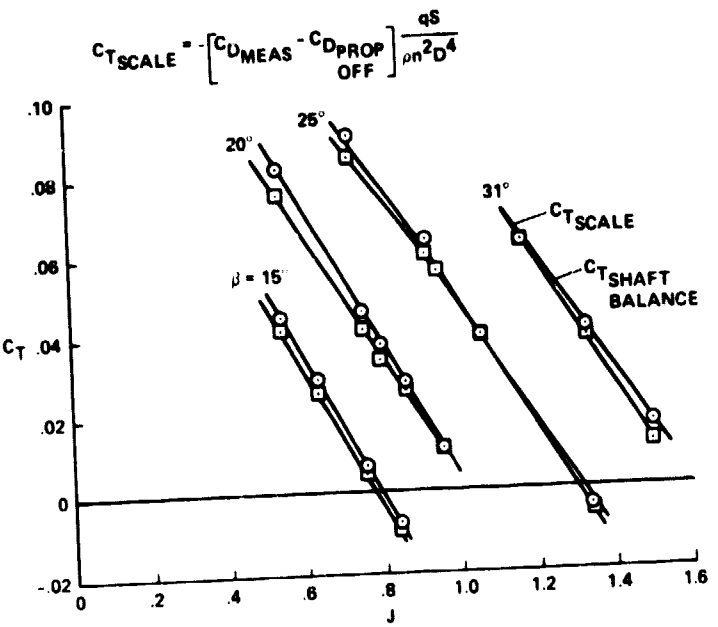

Figure 7.- Comparison of thrust measured on wind-tunnel scales with the corresponding values measured on the shaft balance. Shaft-balance data corrected for spinner drag.

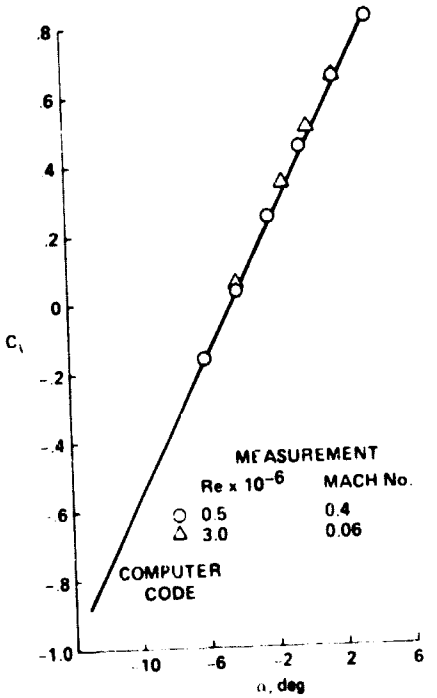

(a) Clark-Y, 10% thick.

Figure 8.- Sectional-lift-coefficient values found in references 7 and 8 compared with the values used in the computer code.

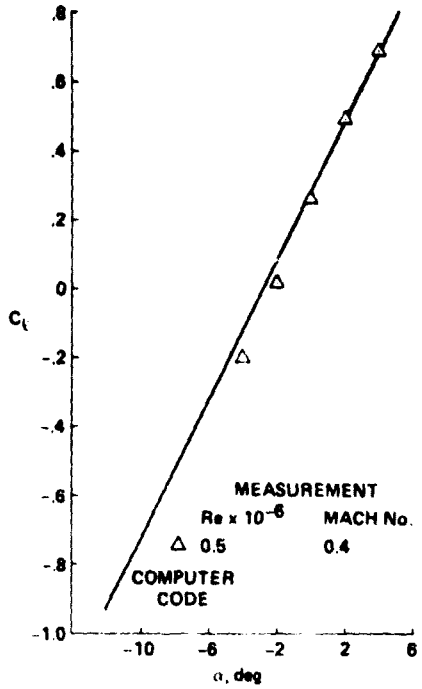

(b) RAF-6, 6% thick.

Figure 8.- Concluded.

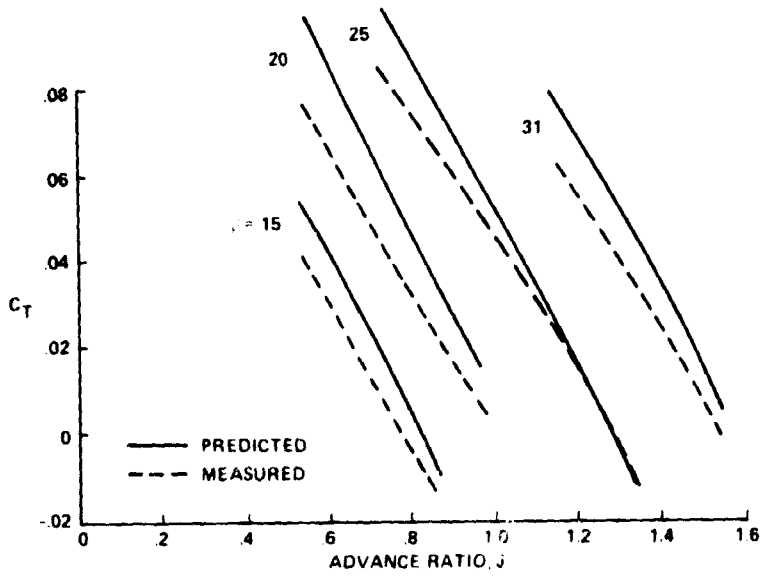

(a) Thrust coefficient.

Figure 9.- Measured propeller performance compared with vortex theory.

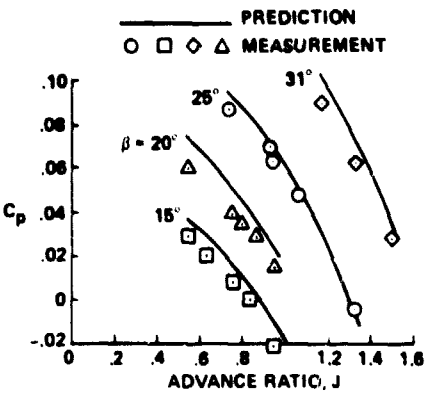

(b) Power coefficient.

Figure 9.- Continued.

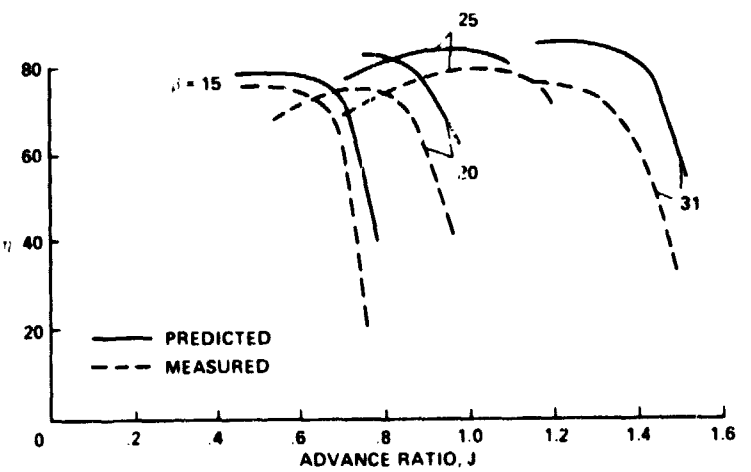

(c) Efficiency.

Figure 9.- Concluded.

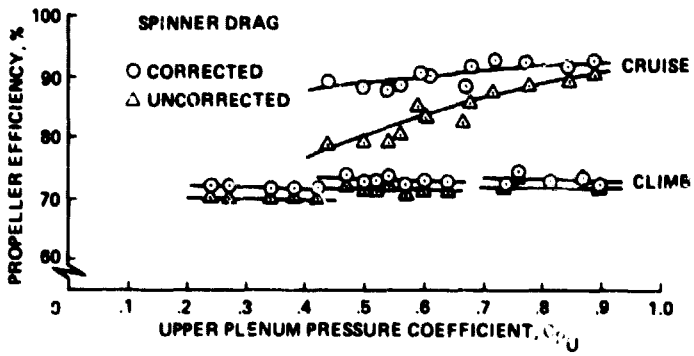

Figure 10.- Measured propeller efficiency as a function of flow rate through the nacelle. Flow rate was varied by changing orifice and cowl-flap opening in the cooling drag portion of the study. Results are shown both with and without the correction for spinner drag. Wing angle of attack = 2.3° (cruise) and 8° (climb).

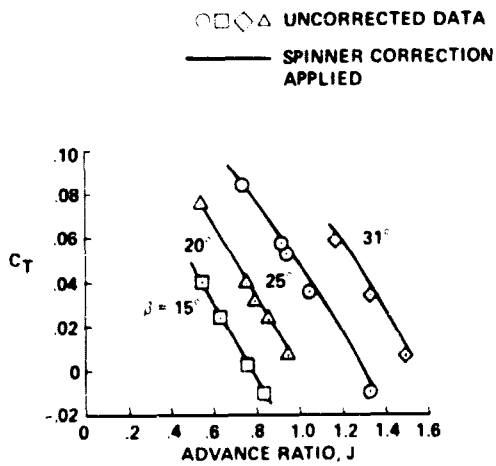

Figure 11.- Measured thrust coefficient with and without the spinner drag correction applied. These data are from the propeller portion of the study in which the orifice and cowl flap were fixed and wing angle of attack was 0°.